Received: 11 July 2019 | Revised: 14 July 2020 | Accepted: 21 July 2020

DOI: 10.1002/joc.6767

RESEARCH ARTICLE

International Journal of Climatology RMetS

Climatic yield potential of Japonica-type rice in the Korean Peninsula under RCP scenarios using the ensemble of multi-GCM and multi-RCM chains

Joong-Bae Ahn[1] | **Young-Hyun Kim**[1] | **Kyo-Moon Shim**[2] | **Myoung-Seok Suh**[3] | **Dong-Hyun Cha**[4] | **Dong-Kyou Lee**[5] | **Song-You Hong**[6] | **Seung-Ki Min**[7] | **Seong-Chan Park**[8] | **Hyun-Suk Kang**[8]

[1]Department of Atmospheric Sciences, Pusan National University, Busan, South Korea

[2]National Academy of Agricultural Science, Wanju, South Korea

[3]Kongju National University, Kongju, South Korea

[4]Ulsan National Institute of Science and Technology, Ulsan, South Korea

[5]Seoul National University, Seoul, South Korea

[6]Korea Institute of Atmospheric Prediction Systems, Seoul, South Korea

[7]Pohang University of Science and Technology, Pohang, South Korea

[8]Korea Meteorological Administration, Seoul, South Korea

Correspondence
Young-Hyun Kim, Division of Earth Environmental System, Pusan National University, 2, Busandaehak-ro 63beon-gil, Geumjeong-gu, Busan, Republic of South Korea.
Email: kyhmaria@pusan.ac.kr

Funding information
Cooperative Research Program for Agriculture Science & Technology Development, Grant/Award Number: PJ01489102; the Korea Meteorological Administration Research and Development Program, Grant/Award Number: KMI2018-01213

Abstract

Rice production in the Korean Peninsula (KP) in the near future (2021–2050) is analysed in terms of the climatic yield potential (CYP) index for Japonica-type rice. Data obtained from the dynamically downscaled daily temperature and sunshine duration for the Historical period (1981–2010) and near future under two Representative Concentration Pathway (RCP4.5 and RCP8.5) scenarios are utilized. To reduce uncertainties that might be induced by using a Coupled General Circulation Model (CGCM)—a Regional Climate Model (RCM) chain in dynamical downscaling, two CGCM—three RCM chains are used to estimate the CYP index. The results show that the mean rice production decreases, mainly due to the increase of the temperature during the grain-filling period (40 days after the heading date). According to multi model ensemble, the optimum heading date in the near future will be approximately 12 days later and the maximum CYP will be even higher than in the Historical. This implies that the rice production is projected to decrease if the heading date is selected based on the optimum heading date of Historical, but to increase if based on that of near future. The mean rice production during the period of ripening is projected to decrease (to about 95% (RCP4.5) and 93% (RCP8.5) of the Historical) in the western and southern regions of the KP, but to increase (to about 104% (RCP4.5) and 106% (RCP8.5) of the Historical) in

the northeastern coastal regions of the KP. However, if the optimum heading date is selected in the near future climate, the peak rice production is projected to increase (to about 105% (RCP4.5) and 104% (RCP8.5) of the Historical) in the western, southern and northeastern coastal regions of the KP, but to decrease (to about 98% (RCP4.5) and 96% (RCP8.5) of the Historical) in the southeastern coastal regions of the KP.

KEYWORDS

climate change, climatic yield potential, multi global climate models, multi model ensemble, multi regional climate models, representative concentration pathways (RCPs), rice production

1 | INTRODUCTION

The average surface air temperature of the earth rose by 0.85°C during the period 1880 to 2012 due to global warming and the rates and magnitudes of warming has been increasing (Intergovernmental Panel on Climate Change, IPCC, 2013). Global warming is unequivocal and its influence on climate and individual subsystems such as the biosphere is evident (IPCC, 2013). The impact of climate change on the ecosystems has already been so severe and widespread throughout the globe that, in particular, food security becomes one of the most daunting human challenges (Gitz *et al*., 2016). According to the World Food Programme (WFP, 2016), the world's famine refugees number approximately 795 million (WFP, 2016) and the Food and Agriculture Organization of the United Nations (FAO) has designated 39 countries in need of external food aid (FAO, 2016b). The global grain inventory rate was also about 16.6% in 2006/2007, lower than the FAO's recommended rate of 18 to 19% (USDA, 2009). According to the average annual food self-sufficiency rate of OECD countries from 2011 to 2013, estimated by the Korea Royal Economic Institute based on FAO statistics, the rates of South Korea and Japan were 21.4 and 24.2%, respectively, which are relatively far lower than other OECD countries (312.3% in Australia, 188.3% in France, 118.7% in the United States, 112.5% in Germany and 100% in China). Therefore, it is essential to estimate future grain production based on projected climate changes for stable crop supply in those 39 countries including OECD countries such as South Korea and Japan.

Several studies have investigated the change in crop production during the past and present periods resulting from climate change using observation data. Shim *et al*. (2008a) insisted that the increase of temperature and decrease of sunshine duration have delayed the beginning date of rice heading in the recent past climate (1988–2006) compared to the more distant past climate (1969–1987) in South Korea using the agro-climate index. Peng *et al*. (2004) argued that the maximum temperature is not directly related to the grain yield, but that a 1°C increase in minimum temperature in the dry cropping season can reduce the grain yield by 10%. Wang and Hijmans (2019) showed that rice yield slightly increased and the average temperature for rice planting area during the rice growing season decreased due to the increased area of rice cultivation in the northern regions of China during 1949–2015.

Recently, many studies demonstrated that the decrease of crop production in the future climate and the uncertainty of climate change impact on crop production using climate change scenarios derived from GCMs. Parry *et al*. (2004) analysed the impacts of climate change on decrease of crop yields (wheat, rice, maize and soybean) and discussed the risk of famine in the future using the projection data of the HadCM3 global climate model under the IPCC Special Report on Emissions Scenarios (SRES) of A1FI, A2, B1 and B2. According to their study, the yield projections under the SRES A1FI scenario are the worst and the SRES scenarios of a more globalized world (A1FI and B1) experience greater reduction in crop yield compared to the scenarios of a more regionalized world (A2 and B2). They also argued that climate change is likely to increase the gaps in cereal yields between developed and developing countries. Deressa and Hassan (2009) argued that climate change would reduce Ethiopian farmer's net revenue by affecting crop farming in Ethiopia using GCMs (CGM2, HADCM3 and PCM). On the other hand, many studies used both multi GCM and crop models to analyse the impacts of climate change on various crop yields under climate change scenarios (SRES, Representative Concentration Pathway scenarios[RCP2.6, RCP3.5, RCP6.0 and RCP8.5]): Bancy (2000) for maize in Kenya; Masutomi *et al*. (2009) and Matthews *et al*. (1997) for rice in Asia; Zhao *et al*. (2015) for six crops (winter wheat, winter barley, rapeseed, grain maize, potato and sugar beet) in

Europe; Wang *et al*. (2017) for rice in China; and Van Oort and Zwart (2017) for rice in Africa.

The spatial resolution of GCM is too coarse to obtain detailed agricultural information by region, particularly in the area of complex topography. In order for climate data simulated by GCM to be used to analyse and predict crop production, the GCM outputs are usually dynamically or statistically downscaled for higher resolutions in space and time. Several recent studies have used a Regional Climate Model (RCM) to dynamically downscale GCM results to high resolution for the present and future climates in the Korean Peninsula. Ahn *et al*. (2016) projected agro-climate changes over Northeast Asia in terms of agro-climate indices (frost days, vegetable periods, crop periods, climatic yield potential (CYP)) based on the RCP scenarios (Historical, RCP4.5 and RCP8.5) using the Weather Research and Forecasting (WRF) model that prescribes the Hadley Centre Global Environmental Model version 2—Atmosphere and Ocean (HadGEM2-AO) simulation data as initial and boundary conditions. According to their results, the future rice production will decrease because optimum grain-filling periods will be delayed and the possible period of rice ripening will be decreased despite the rice growing period being increased due to the decreased number of frost days and the increased vegetable and crop periods. Meanwhile, Ahn *et al*. (2014) analysed downscaled data by HadGEM2-AO and WRF chain for summer temperatures and precipitations during the Historical period (1981–2005) to prove the feasibility of detailed climate data simulated by the WRF. Hong *et al*. (2013a) also used an RCM, RegCM4, to produce high resolution climate data in Northeast Asia for the Historical period and compare it with the Climate Research Unit (CRU) observations to verify the validity of the downscaled data.

Although some studies have projected future crop production with high resolution regional model data dynamically downscaled from CGCM simulations, the biases and uncertainties of the model results have not been taken into account because these results were obtained from a single CGCM and a single RCM chain. Ensemble prediction using multiple models has generally proven to be more reliable, skillful and consistent than single-model prediction (Tebaldi and Knutti, 2007). Hur *et al*. (2017) used daily temperature data that were dynamically downscaled through one CGCM (Hadley Center Global Environmental Model version 3, HadGEM3)—five RCMs (WRF version 4.3.4, RegCM4; HadGEM3-RA; Seoul National University Meso-scale Model version 5, SNU-MM5; Global/Regional Integrated Model system, GRIMs) chain to project the first-day of cherry blossoms under warmed climate. Although the study used multi-RCM results for their analysis to reduce the uncertainties and bias of the model simulation, they still may not have eliminated the uncertainty and bias that could result from using a single CGCM.

The objective of this study is to produce more reliable and fine resolution projection for rice production in the near future (2021–2050) in the Korean Peninsula (33–43°N, 124.5–130°E) using multi GCMs and multi RCMs ensemble. We project the change in CYP for Japonica-type rice (hereafter, rice), one of the main varieties of rice produced and consumed in this region, using the Historical (hereafter, HS), RCP4.5 and RCP8.5 scenarios.

2 | MODEL AND DATA

In this study, two GCMs (HadGEM2-AO, European Centre/Hamburg model version 6[ECHAM6]) and three RCMs (WRF, SNU-MM5, GRIMs) are used to estimate the rice production change in the Korean peninsula under the RCP scenarios. Global-scale simulations by HadGEM2-AO and ECHAM6 provided by the National Institute of Meteorological Research/Korea Meteorological Administrations (NIMR/KMA) are used as the initial and lateral boundary conditions of the RCMs, respectively. The WRF and SNU-MM5, which use the lateral forcing from HadGEM2-AO, are denoted as HGM_WRF and HGM-MM5, respectively, and their ensemble mean as HGM_MME. Likewise, ECH_WRF and ECH_GRIMs denote chains of WRF and GRIMs which use the lateral forcing from ECHAM6, respectively, and ECH_MME as the ensemble mean of the two. Lastly, the ensemble mean of all (HGM_WRF, HGM_MM5, ECH_WRF, ECH_GRIMs) is denoted by ALL_MME. In this study, GCM projections that are dynamically downscaled using RCM are named as GCM-RCM chains. Seven cases of GCM-RCM chains (HGM_WRF, HGM_MM5, ECH_WRF, ECH_GRIMs, HGM_MME, ECH_MME, ALL_MME) are shown in Figure 1.

Spatial and temporal resolutions of HadGEM2-AO (ECHAM6) data are 1.875° × 1.250° (1.86° × 1.86°) and 6 hr (6 hr). A detailed description of HadGEM2-AO and ECHAM6 is provided in Collins *et al*. (2011) and Stevens *et al*. (2013), respectively. The horizontal resolution of the RCMs is 12.5 km, the map projection is the Lambert conformal type, and the model has the domain of 110.6–144.38°E, 26.56–47.90°N (Figure 2). The configuration of the RCMs is summarized in Table 1.

The analysis periods are for the Historical period 1981–2010 and 2021–2050 for the near future. The analysis variables are daily mean temperature (°C) and daily sunshine duration (hours). The daily sunshine duration for each grid was estimated by accumulating the duration

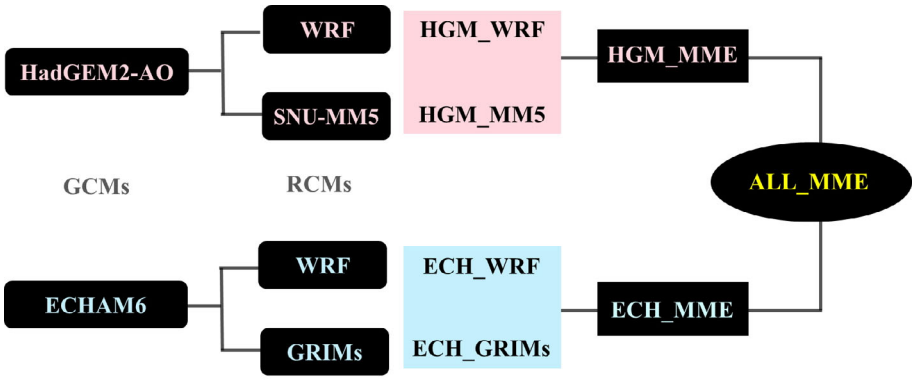

FIGURE 1 GCM-RCM chain and its ensemble [Colour figure can be viewed at wileyonlinelibrary.com]

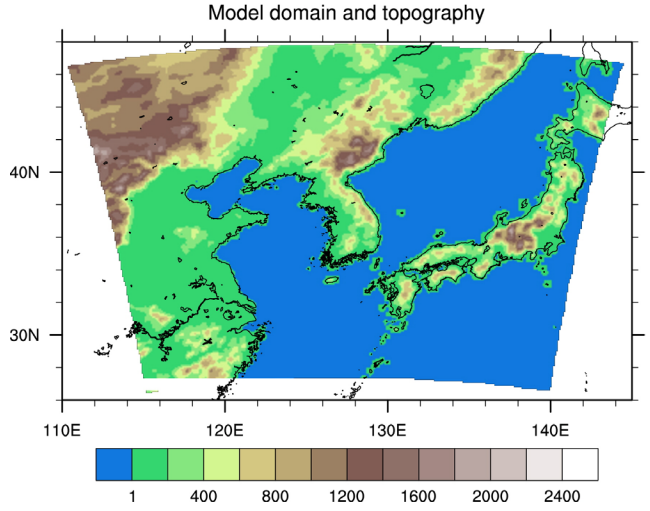

FIGURE 2 Model domain and topography (m) [Colour figure can be viewed at wileyonlinelibrary.com]

when the hourly incident shortwave radiation (SR) is greater than zero and the hourly precipitation is zero at each grid (Ahn *et al*., 2016).

In order to project the rice production change, the CYP index for Japonica, the major crop cultivated in Korea, northeastern China and Japan, is used. CYP is defined as follows.

$$\mathrm{CYP}\left(\mathrm{kg}/10^3\,\mathrm{m}^2\right) = DS\left(\alpha - \beta\left(T_\mathrm{a} - T_1\right)^2\right) \qquad (1)$$

where DS is the daily accumulated sunshine duration and T_a the average surface air temperature during the 40 days after the heading date. T_1 (21.4°C) is the most proper mean temperature for rice during the grain-filling period and α (4.14) and β (0.13) are regression coefficients, which can be changed depending on the variety of rice (Hanyu *et al*., 1966; Ahn *et al*., 2016). According to the Korea Rural Development Administration (RDA) (2004, 2019) and Han (2016), the optimum temperature range is 20–22°C during the grain-filling period for high quality rice production in South Korea. Thus, T1 (21.4°C) remains within the range of optimum temperature for rice production. In this study, α and β are assigned as 4.14 and 0.13, respectively, to analyse CYP for Japonica-type rice. As rice varieties are developed to mitigate the damage caused by climate change, the regression coefficient may change. However, the development of rice varieties to prepare for future climate change have been focused on Japonica-type rice in Korea (Park *et al*., 2017, 2018; Jeong *et al*., 2019) because Koreans prefer Japonica-type rice (Choi, 2002; Park *et al*., 2017, 2018). Therefore, these parameters in Equation (1) have been used in many recent studies that estimated CYP for Japonica-type rice in South Korea (e.g., Son *et al*., 2002; Kim *et al*., 2007; Seo *et al*., 2010; Lee *et al*., 2014; Ahn *et al*., 2016). If CYP of the heading dates is larger than 0, the temperatures and sunlight that are given for 40 days after the heading date are suitable for ripening of the rice. The optimal seeding date for rice in the Korean Peninsula is from late April to late May (Lee *et al*., 2012b; Kim *et al*., 2013; Ahn *et al*., 2016) and the heading date is from 70.6 to 109.3 days after the seeding date (Wei *et al*., 2008, 2009; Ahn *et al*., 2016). Accordingly, the earliest heading date is July 1, being 71 days after the earliest optimal seeding date (April 21), and the latest heading date is September 18, being 110 days after the latest optimal seeding date (May 31). Considering these and following Ahn *et al*. (2016), 1 July to 18 September is selected as the heading date period of the rice in this study. In order to verify that the CYP defined in this study (Hanyu *et al*., 1966) can be applied to Korea in the present climate (1981–2010), the actual rice production in South Korea (RP_OBS) provided by the Korean Statistical Information Service (KOSIS) was compared with rice production calculated using the CYP index (RP_CYP) during the 30-year period of 1981–2010. RP_CYP was obtained by multiplying the annual rice cultivation area provided by KOSIS and the average CYP during the heading date calculated from the mean temperature and sunshine duration observed by KMA at 60 stations. Both RP_OBS and

TABLE 1 Model configuration used in this study

	WRF	SNU-MM5	GRIMs
Horizontal resolution	12.5 km	12.5 km	12.5 km
Vertical level Eta-28	σ − 24	σ − 28	
Dynamic framework	Non-hydrostatic	Non-hydrostatic	Hydrostatic
Microphysics scheme	WSM3	Reisner2	WSM1
PBL scheme	YSU	YSU	YSU + stable BL
Convection scheme	Karin-FritschII	Karin-FritschII	SAS + CMT
Land surface	NOAA	CLM3.0	OML-climatology
Radiation scheme	CAM	CCM2	GSFC
Spectral nudging	No	Yes	Yes
Reference	Ahn *et al*. (2016)	Lee *et al*. (2004)	Hong *et al*. (2013b)

RP_CYP are detrended. RP_CYP is the potential rice yield at a given temperature and sunshine duration, while RP_OBS can be affected by not only temperature and sunshine duration but also disease or pests and extreme weather disasters such as heatwaves, flood and drought. Therefore, RP_CYP and actual rice production in South Korea provided by the KOSIS (RP_OBS) can be different. Nevertheless, the correlation coefficient between RP_OBS and RP_CYP is about 0.39, which was significant at the 95% confidence level. This implies that the CYP defined in this study can be effectively used for analysing the impact of changes in temperature and sunshine duration that are important factors determining rice ripening (Kim, 2010; Lee *et al*., 2016) on changes in rice yield in the Korean Peninsula in the near future.

To verify both CYP index and the distribution of surface air temperature and sunshine duration simulated by the GCM-RCM chain, 60 observational in-situ stations data (Automated Synoptic Observing System, ASOS) provided by KMA are used.

3 | RESULTS

3.1 | Evaluation of the annual mean surface air temperature and sunshine duration simulation for present climate

In order to validate the general performance of the RCMs, the spatial distributions of annual mean surface air temperature and annual mean sunshine duration of four RCMs (HGM_WRF, HGM_MM5, ECH_WRF, ECH_GRIMs) and ALL_MME for the HS run are compared with those of the in situ observation data (OBS) provided by KMA at 60 stations. For comparison with the station data, the gridded surface air temperature and sunshine duration simulated by four RCMs and ALL_MME are interpolated into 60 stations. Figure 3a–f displays the observed temperature of OBS and simulated 30-year mean surface air temperature of four RCMs (HGM_WRF, HGM_MM5, ECH_WRF, ECH_GRIMs) and ALL_MME for the HS run, respectively. The mean surface air temperature is higher in the southern (eastern) part than in the northern (western) part of South Korea in OBS, four RCMs and ALL_MME. These mean that climatological characteristic of temperature according to latitude and altitude are as well represented in four RCMs and ALL_MME as in OBS. For example, the southern (western) part of the Korean peninsula is warmer than the northern (eastern) part. The area-averaged climatology (1981–2010) of annual mean surface air temperature is 12.6, 11.6, 11.6, 12.2, 10.8 and 11.6°C in OBS (Figure 3a), HGM_WRF (Figure 3b), HGM_MM5 (Figure 3c), ECH_WRF (Figure 3d), ECH_GRIMs (Figure 3e) and ALL_MME (Figure 3f), respectively. The difference is because four RCMs and ALL_MME underestimate the temperatures compared to the observed temperatures in southeastern part of the South Korea and eastern part of the South Korea where mountain ranges are located (see Figure 2). Overall, the temperature of four RCMs and ALL_MME are distributed over a similar range to that of OBS. Figure 3g–l displays the observed sunshine duration of OBS and simulated 30-year mean sunshine duration of four RCMs and ALL_MME for the HS run, respectively. The distributions of sunshine duration in OBS, four RCMs and ALL_MME do not show any regional characteristics that are clearly shown in the distributions of temperature. The area-averaged climatology (1981–2010) of annual mean surface air temperature is 6.1, 8.0, 8.3, 7.1, 6.2, and 7.4 hr in OBS (Figure 3g), HGM_WRF (Figure 3h), HGM_MM5 (Figure 3i), ECH_WRF (Figure 3j), ECH_GRIMs (Figure 3k) and ALL_MME (Figure 3l), respectively. Four RCMs and ALL_MME overestimate

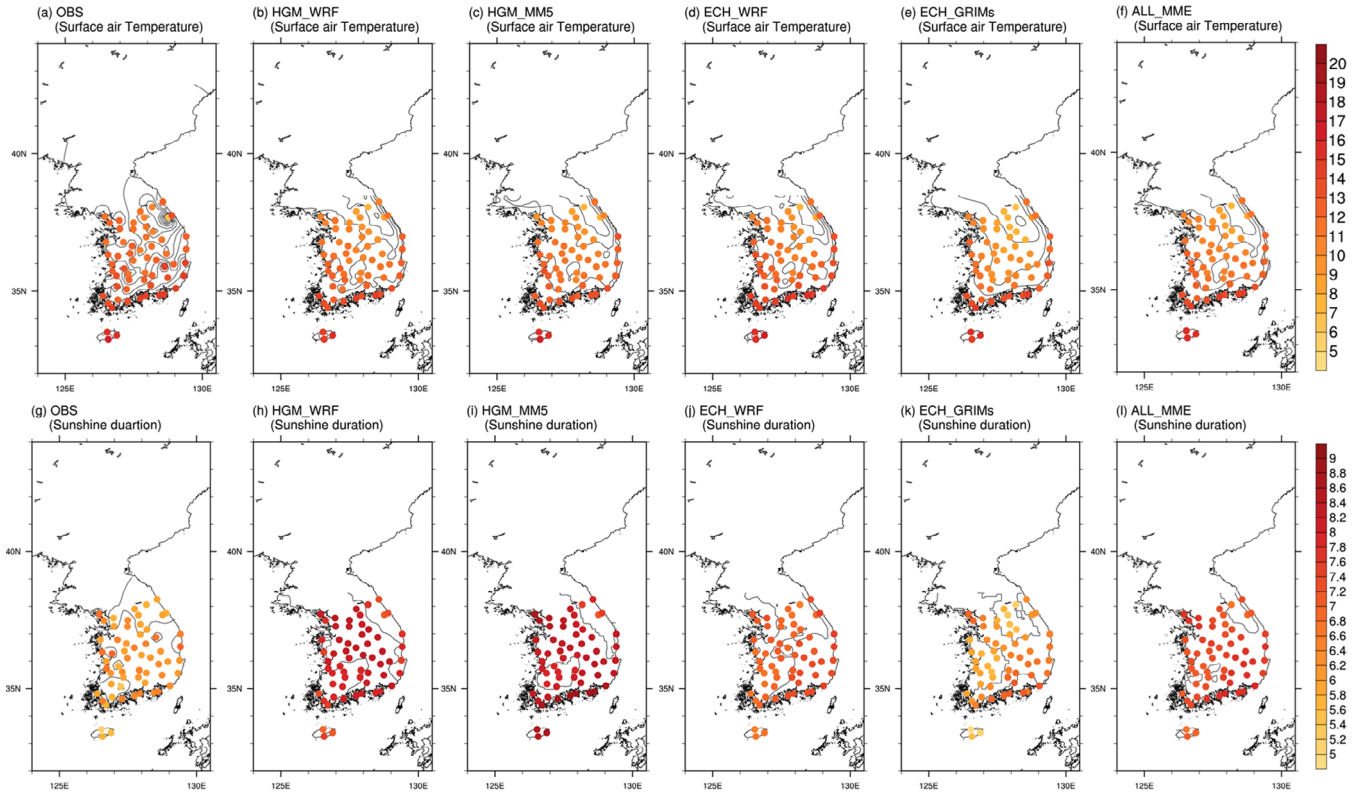

FIGURE 3 Distributions of annual mean surface air temperature (°C) and annual mean sunshine duration (hr) over 30 years (1981–2010) derived from four RCMs (HGM_WRF, HGM_MM5, ECH_WRF, ECH_GRIMs) and ALL_MME for the HS run (b–f and h–l) and the observation data (OBS) observed by KMA at 60 stations (a and g) [Colour figure can be viewed at wileyonlinelibrary.com]

the sunshine duration than observed sunshine duration in most regions of South Korea. But as with OBS, the distribution of sunshine duration represents a similar range without much regional difference. The surface air temperature and sunshine duration for the HS run by four RCMs and MME are overall properly simulated compared to those of the OBS. Figure 4 shows the normalized standard deviation (NSD) and root mean square error (RMSE) of annual mean surface air temperature and annual mean sunshine duration over 30 years (1981–2010) derived from four RCMs and ALL_MME. The NSD of annual mean surface air temperature is 0.92, 0.87, 0.91, 1.27 and 0.78 in HGM_WRF, HGM_MM5, ECH_WRF, ECH_GRIMs and ALL_MME, respectively. As they are close to 1.0, they indicate that mean surface air temperature simulated by four RCMs and ALL_MME well represent the temporal variation of OBS. The RMSE of annual mean surface air temperature is 1.22, 1.29, 0.96, 2.19 and 1.33 in HGM_WRF, HGM_MM5, ECH_WRF, ECH_GRIMs and ALL_MME, respectively. Among the RCMs, ECH_WRF (ECH_GRIMs) has minimum (maximum) RSME and NSD of ECH_WRF (ECH_GRIMs) is the closest to (farthest from) 1.0. The NSD of annual mean sunshine duration is 0.60, 0.46, 0.59, 0.69 and 0.39 in HGM_WRF, HGM_MM5, ECH_WRF, ECH_GRIMs and ALL_MME, respectively. The annual mean sunshine duration simulated by four RCMs and ALL_MME does not well represent the temporal variation of OBS compared to the annual mean surface air temperature. The RMSE of the annual mean surface air temperature is 1.89, 2.22, 1.00, 0.53 and 1.31 hr in HGM_WRF, HGM_MM5, ECH_WRF, ECH_GRIMs and ALL_MME, respectively. Among the RCMs, ECH_GRIMs (HGM_MM5) has minimum (maximum) RSME and NSD of ECH_GRIMs (ALL_MME) is the closest to (farthest from) 1.0. Among these analyses, the RCM results including ALL_MME show a reasonable performance.

3.2 | Domain area-averaged CYP with respect to heading date

Figure 5 shows the spatial distributions of CYP climatology for HS (1981–2010) and RCPs (2021–2050). The black-coloured area, where CYP is lower than 0, denotes the impossibility of producing rice. The area of possible rice production is expanded in the near future. However,

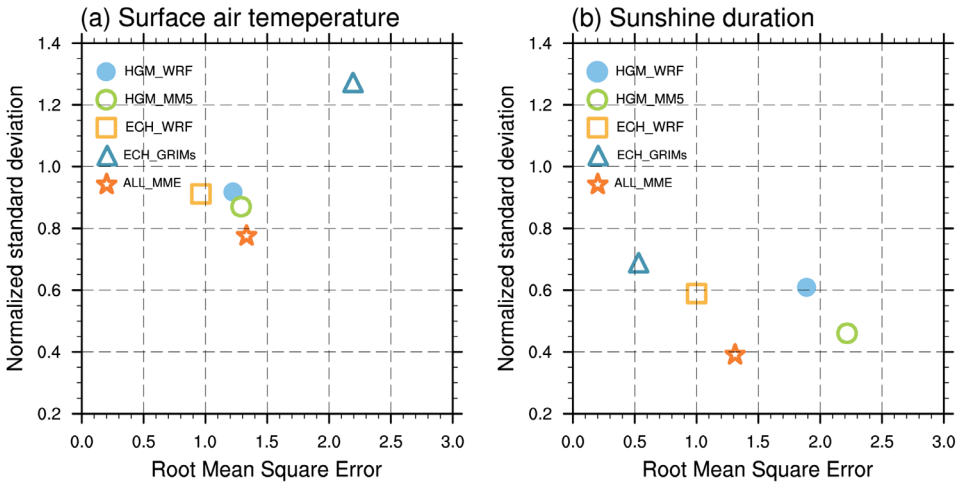

FIGURE 4 Normalized standard deviation and root mean square error of annual mean surface air temperature (°C) (a) and annual mean sunshine duration (hours) (b) over 30 years (1981–2010) for four RCMs and ALL_MME [Colour figure can be viewed at wileyonlinelibrary.com]

most of the areas of possible future rice production are mountainous forest regions, where rice cannot be practically produced. Accordingly, in the further analyses of RCP4.5, and in the RCP8.5 results, the black area (CYP is lower than 0) in the HS result is excluded (Figure 5a).

A time series of domain-averaged CYPs for the HS, RCP4.5 and RCP8.5 scenarios with respect to heading dates is shown in Figure 6. For example, CYP for a heading date of August 1 is determined by Equation (1) for 40 days from 2 August to 10 September (Ahn *et al*., 2016). Figure 6a–d shows the results of HGM_WRF, HGM_MM5, ECH_WRF and ECH_GRIMs, where the black, blue and red solid lines denote the HS, RCP4.5 and RCP8.5 scenarios, respectively. The results of HGM_WRF, HGM_MM5, ECH_WRF, ECH_ GRIMs and ALL_MME are represented together for the RCP4.5 (Figure 6e) and RCP8.5 (Figure 6f) scenarios. In these panels, the dashed and solid lines denote the HS and RCPs scenarios. The blue, black, green, yellow and red curves indicate HGM_WRF, HGM_MM5, ECH_WRF, ECH_ GRIMs and ALL_MME, respectively.

CYPs based on the HS scenario (HS_CYP, hereafter) derived from HGM_WRF (Figure 6a) show gradual increases from early July to reach a maximum peak in mid August, after which HS_CYP decreases and drops below 0 with heading dates of after mid September. All of the HS_CYPs derived from HGM_MM5, ECH_WRF, ECH_GRIMs and ALL_MME (Figure 6b–f) slightly decrease from early to mid July and then increase to their maximums at the time when the heading date is early to mid August. HS_CYP decreases rapidly with heading dates of early to mid August and eventually becomes 0 when the heading dates are around mid September. The optimum heading dates (when CYP is maximum) of HS_CYP are about mid August for every model [7 August (HGM_WRF), 17 August (HGM_MM5), 10 August (ECH_WRF), 8 August (ECH_GRIMs), 10 August (ALL_MME)]. These results are consistent with the preceding studies (Shim *et al*., 2008a; Ahn *et al*., 2016), which suggested that the optimum heading date period for rice cultivars in the central regions of the Korean Peninsula is from early to late August. During all the heading date periods, the HS_CYP derived from HGM_WRF (Figure 6a) and HGM_MM5 (Figure 6b) is higher than that derived from ECH_WRF (Figure 6c) and ECH_GRIMs (Figure 6d), indicating that the difference is basically derived from the GCMs used as boundary conditions.

In the RCPs result, CYPs derived from 4 RCMs and ALL_MME decrease until mid July, and then they increase and reach their maximum when the heading date is mid or late August. CYP of the RCPs scenarios (RCPs_CYP, hereafter) decreases and becomes 0 when the heading date is mid or late September. The variation of RCPs_CYP is larger than that of HS_CYP, which is almost constant until mid August. In HGM_WRF (Figure 6a) and HGM_MM5 (Figure 6b), CYP of the RCP8.5 scenario (RCP8.5_CYP, hereafter) is higher than that of the RCP4.5 scenario (RCP4.5_CYP, hereafter) until mid July and lower than that until late August or early September. The heading date of RCP8.5_CYP when CYP begins to increase is about 5 days later than that of RCP4.5_CYP. The difference between the HGM_WRF-driven RCPs_CYP (Figure 6a) and the HGM_MM5-driven RCPs_CYP (Figure 6b) until the optimum heading date is based on the RCM used because the initial and lateral boundary conditions of both HGM_WRF and HGM_MM5 are HadGEM2-AO. For ECH_WRF (Figure 6c) and ECH_GRIMs (Figure 6d), RCP8.5_CYP is lower (higher) than RCP4.5_CYP until (after) late August. The trend of RCP4.5_CYP is similar to that of RCP8.5_CYP. Although RCM is different, the differences between the distribution of RCPs_CYP derived from ECH_WRF (Figure 6c) and that of RCPs_CYP derived

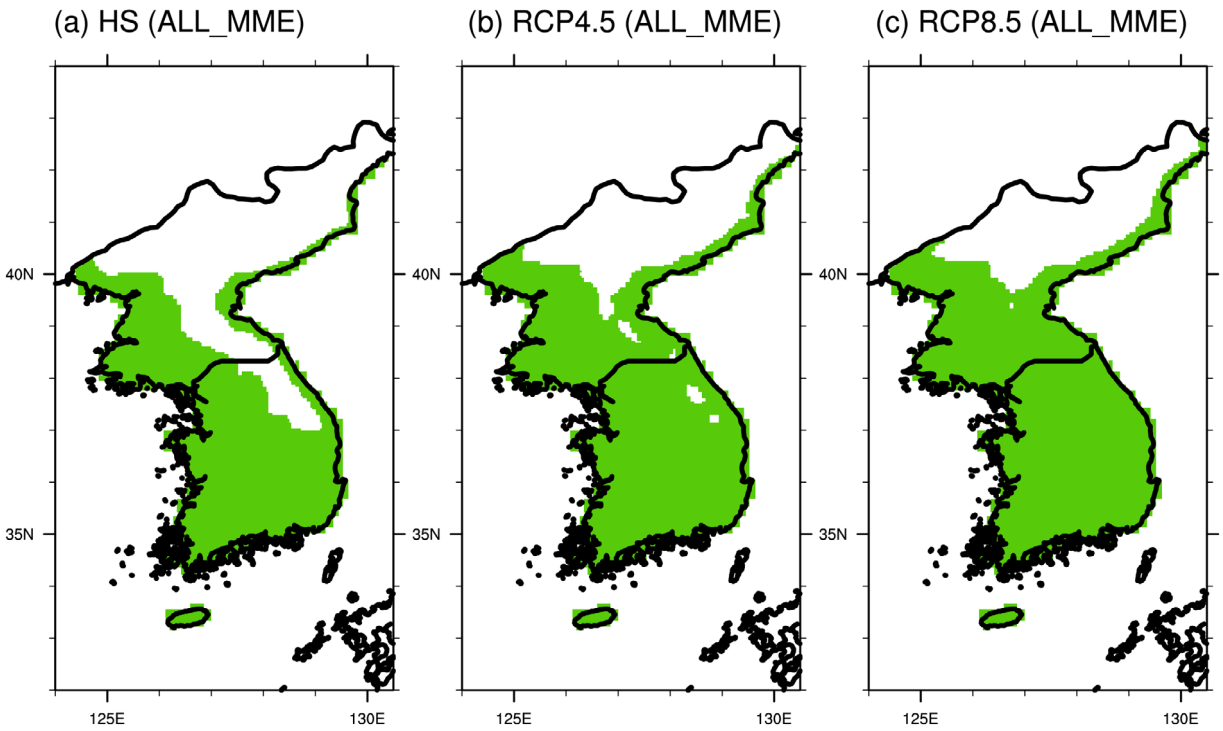

FIGURE 5 Spatial distribution of CYP climatology (HS: 1981–2010, RCP: 2021–2050) from ALL_MME for (a) HS, (b) RCP4.5 and (c) RCP8.5 runs. The black (green)-coloured area is where rice production is impossible (possible) [Colour figure can be viewed at wileyonlinelibrary.com]

from ECH_ GRIMs (Figure 6d) are not large. In ALL_MME (Figure 6e,f), both RCP4.5_CYP and RCP8.5_CYP are lower than HS_CYP until mid August but higher than that thereafter. The maximum of CYP increases and the optimum heading date is delayed in RCPs_CYP compared to HS CYP. The possible period of rice ripening of RCP_CYP is longer than that of HS_CYP as well.

Table 2 displays the possible period of rice ripening, mean CYP for positive CYP, CYP on the date of the optimum heading date of HS_CYP, the peak of CYP, and the optimum heading dates shown in Figure 6 for the RCMs and ALL_MME. The possible period of rice ripening for the RCP scenarios is projected to be extended by about a week compared with HS, because the heading date when CYP becomes negative has been delayed by about a week. However, the average rice production is projected to decrease in comparison with that of the HS result because the mean RCPs_CYP is lower than the mean HS_CYP. If the heading date is selected as the optimum heading date of HS_CYP, the rice production is projected to decrease because RCPs_CYP is lower than HS_CYP on the date when HS_CYP is the maximum. However, if the heading date is selected as the projected optimum heading date of RCPs_CYP that appears about 12 days (ALL_MME) later than that of HS_CYP, the rice production is expected to increase in the near future because the peak of RCPs_CYP is higher than that of HS_CYP on the date of the optimum heading date in RCPs_CYP.

3.3 | Changes in mean CYP during the heading date

Figure 7 shows the differences in mean CYP between the HS and RCP scenarios during the possible period of rice ripening (when CYP is more than zero) to explore the change of the regional mean rice production in the future climate. By removing CYP of HS from CYP of the RCP scenarios, much of the systematic model bias can be removed according to many previous studies (e.g., Chen and Sun, 2013; Gao *et al*., 2013; Oh *et al*., 2014; Hong and Ahn, 2015; Ahn *et al*., 2016). The black areas in the figures are the regions where rice production is impossible for the same reason is explained in Figure 5a. In HGM_MME (Figure 7a,b), RCPs_CYP increases in the northeastern coastal regions of the Korea Peninsula and decreases in most of other regions, especially in Jeju Island where it decreases by more than 300 kg/10^3 m^2. RCP8.5_CYP largely decreases compared to RCP4.5_CYP and the area in which RCP8.5_CYP increases are extended to the eastern coastal regions compared to that of RCP4.5_CYP. In ECH_MME (Figure 7c,d), there are no changes in most the inland area, but rice production

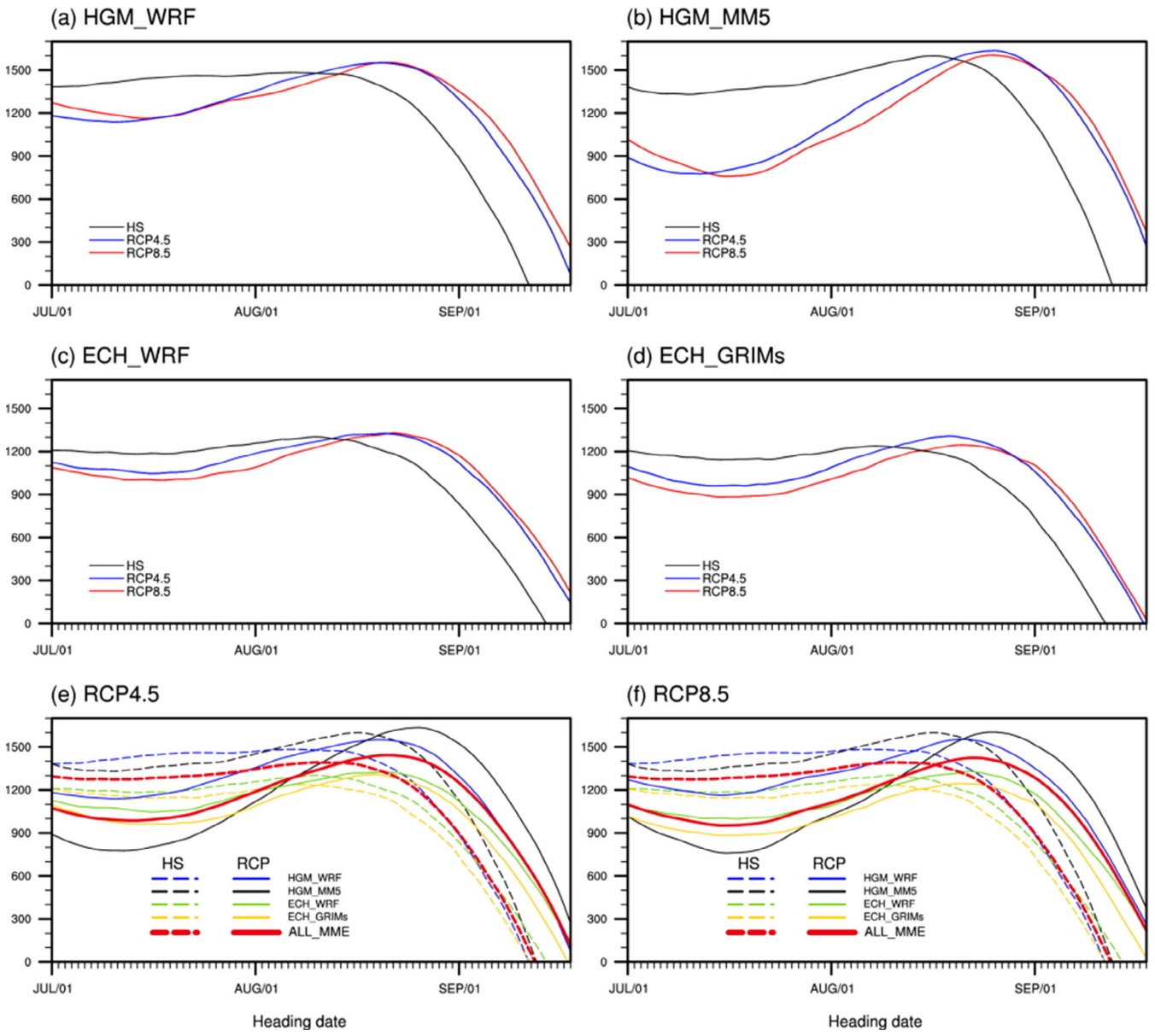

FIGURE 6 Times series of domain area-averaged CYP with respect to heading dates for the HS, RCP4.5 and RCP8.5 scenarios [Colour figure can be viewed at wileyonlinelibrary.com]

decreases in the western and southern parts of the Korean Peninsula and Jeju Island. The RCPs_CYP increases in the northeastern coastal regions of the Korean Peninsula but this increase is less than that of HGM_MME. Finally in ALL_MME (Figure 7e,f), mean rice production during the possible period of rice ripening is projected to increase in the northeastern coastal regions of the Korean Peninsula where mean CYP increases and mean rice production is projected to decrease in the western and southern parts of the Korean Peninsula and Jeju Island, where mean CYP decreases. Especially, RCP8.5_CYP decreases by more than 100 kg/10^3m^2 in the southern regions including the major granary of South Korea and Jeju Island.

In order to investigate the causes of mean CYP changes, we examine changes (RCPs minus HS results) in the square mean differences of T_a and T_1 (TS.CYP) and DS (DS.CYP) averaged over the heading date derived from ALL_MME (Figure 8). TS.CYP decreases in the northeastern coastal regions of the Korean Peninsula where mean CYP increases. TS.CYP increases in the western and southern parts of the Korea Peninsula and Jeju Island where mean CYP decreases. In RCP8.5, the area in which TS.CYP decreases is extended to the eastern coastal regions. Also TS.CYP of RCP8.5 increases more in the southern regions, including the major granary of South Korea, than that of RCP4.5. For RCP4.5, DS.CYP increases in most regions except the eastern

TABLE 2 The possible period of rice ripening, mean CYP for positive CYP, CYP on the date of the optimum heading date of HS_CYP, peak of CYP and optimum heading dates

MODEL	Scenario	Possible date (CYP > 0)	Mean CYP ($kg/10^3 m^2$)	CYP (when HS CYP is maximum)	Maximum CYP ($kg/10^3 m^2$)	Maximum CYP date
HGM_WRF	HS	Sep 11	1,265	1,483	1,483	Aug 7
	RCP4.5	Sep 18	1,208	1,444	1,550	Aug 13
	RCP8.5	Sep 18	1,236	1,381	1,553	Aug 16
HGM_MM5	HS	Sep 12	1,309	1,599	1,599	Aug 17
	RCP4.5	Sep 18	1,126	1,528	1,636	Aug 26
	RCP8.5	Sep 18	1,109	1,455	1,604	Aug 25
ECH_WRF	HS	Sep 14	1,065	1,303	1,303	Aug 10
	RCP4.5	Sep 18	1,067	1,267	1,325	Aug 21
	RCP8.5	Sep 18	1,051	1,225	1,328	Aug 22
ECH_GRIMs	HS	Sep 11	1,038	1,238	1,238	Aug 8
	RCP4.5	Sep 17	1,003	1,203	1,309	Aug 19
	RCP8.5	Sep 18	951	1,119	1,246	Aug 21
ALL_MME	HS	Sep 12	1,168	1,392	1,392	Aug 10
	RCP4.5	Sep 18	1,098	1,334	1,443	Aug 21
	RCP8.5	Sep 18	1,086	1,262	1,425	Aug 23

coastal regions and the inland areas of Jeju Island. Especially, DS.CYP increases by more than 11 hr in the western regions of the Korean Peninsula. For RCP 8.5, DS.CYP increases in the western part of the Korean Peninsula where mean CYP decreases and DS.CYP increases more in the northeastern coastal regions where mean CYP increases. However, there are few changes in DS.CYP in the southern part of the Korean Peninsula and Jeju Island, where mean CYP decreases more. In summary, mean CYP decreases in most western and southern regions of the Korean Peninsula and Jeju Island, where TS.CYP increases and DS.CYP increases or remains unchanged. Mean CYP increases in the northeastern coastal regions of the Korean Peninsula, where TS.CYP decreases and DS.CYP increases. Mean CYP decreases when TS.CYP increases and DS.CYP increases or does not change in the southern and western parts of the Korean Peninsula and Jeju Island. However, mean CYP increases when DS.CYP also increases but TS.CYP decreases in the northeastern part of the Korean Peninsula. Therefore, mean CYP is more affected by TS.CYP than by DS.CYP. As seen from Equation (1), if temperature increases, CYP decreases because the difference between the average temperature during 40 days after the heading date (T_a) and the most proper mean temperature for rice during the grain-filling period (T_1, 21.4°C) increases.

3.4 | Changes in maximum CYP during the heading date

Figure 9 shows the changes in maximum CYP for the optimum heading date (the date when CYP is maximum). In HGM_MME, the maximum of RCP4.5_CYP (Figure 9a) increases in most other regions except the northwestern regions of the Korea Peninsula and decreases in the southern coastal area of the Korean Peninsula and Jeju Island. The maximum of RCP8.5_CYP (Figure 9b) increases significantly only in the eastern regions of the Korean Peninsula and decreases in the southern coastal area and Jeju Island. Especially, those increase by more than 150 $kg/10^3m^2$ in the northeastern coastal regions of the Korean Peninsula. The maximum of RCP8.5_CYP decreases in the southern coastal area and Jeju Island and increases in the eastern coastal regions of the Korean Peninsula is the same as that of RCP4.5_CYP. However, the differences between HS_CYP and RCP8.5_CYP are larger than those between HS_CYP and RCP4.5_CYP in the northeastern coastal regions of the Korean Peninsula and Jeju Island. For ECH_MMM, the maximum of RCP4.5_CYP (Figure 9c) increases in the western and southern parts and some parts of the eastern coastal regions of the Korean Peninsula, but there are no significant changes in RCP4.5_CYP in other regions. The maximum of RCP8.5_CYP (Figure 9d) increases in the

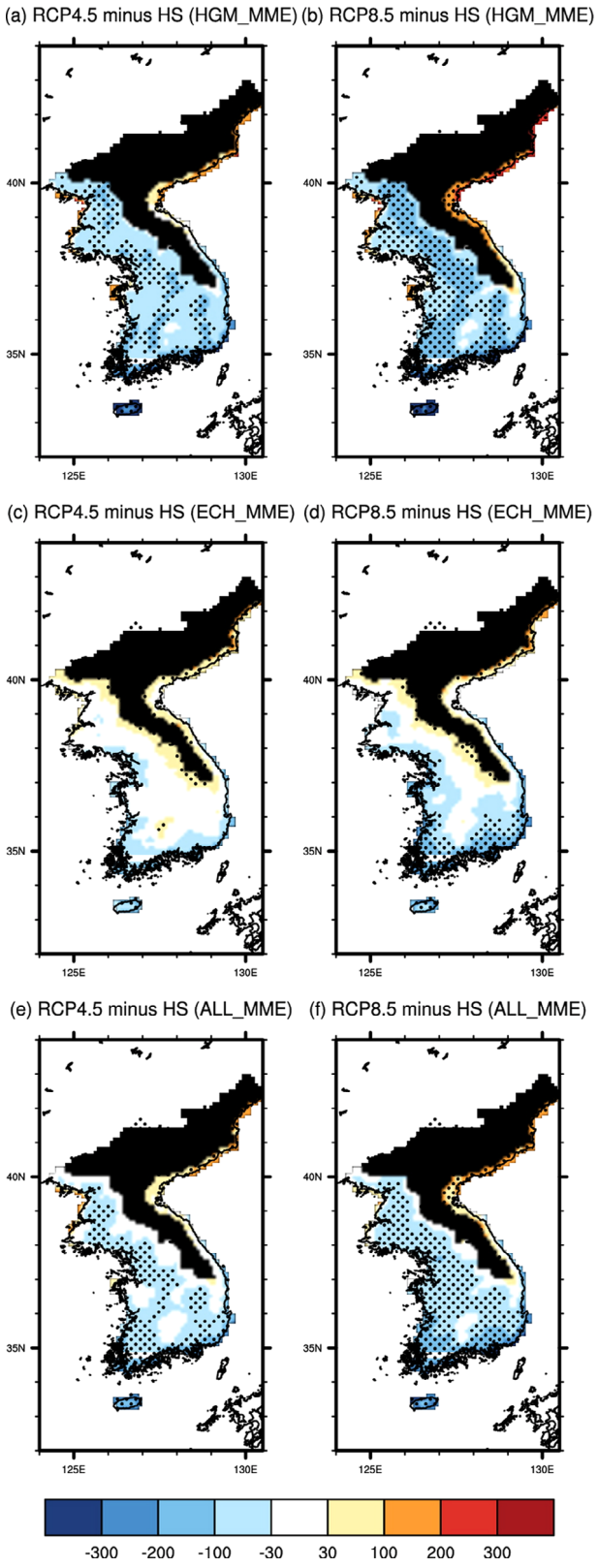

FIGURE 7 Differences in mean CYP (kg/10^3 m^2) during the heading date between HS and RCPs. The left (right) panels indicate the differences between the HS and RCP4.5 (RCP8.5) runs. Grid points with black dots denote the 95% confidence level based on the Student's *t* test [Colour figure can be viewed at wileyonlinelibrary.com]

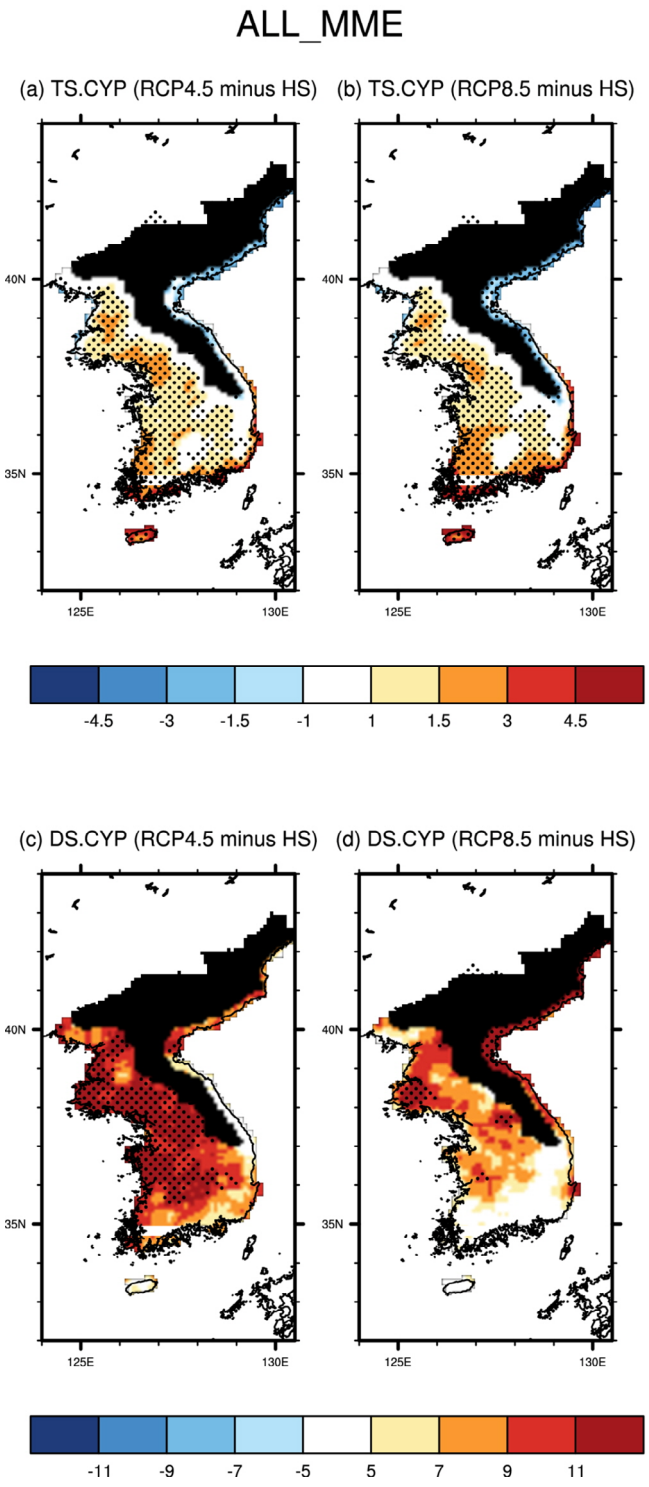

FIGURE 8 Differences in TS.CYP (°C) and DS.CYP (hr) during the heading date between HS and RCPs. The left (right) panels indicate the differences between the HS and RCP4.5 (RCP8.5) runs. Grid points with black dots denote the 95% confidence level based on the Student's *t* test [Colour figure can be viewed at wileyonlinelibrary.com]

western part of the Korean Peninsula and decreases in the southeastern coastal regions of the Korean Peninsula and Jeju Island. For ALL_MME, the maximum of

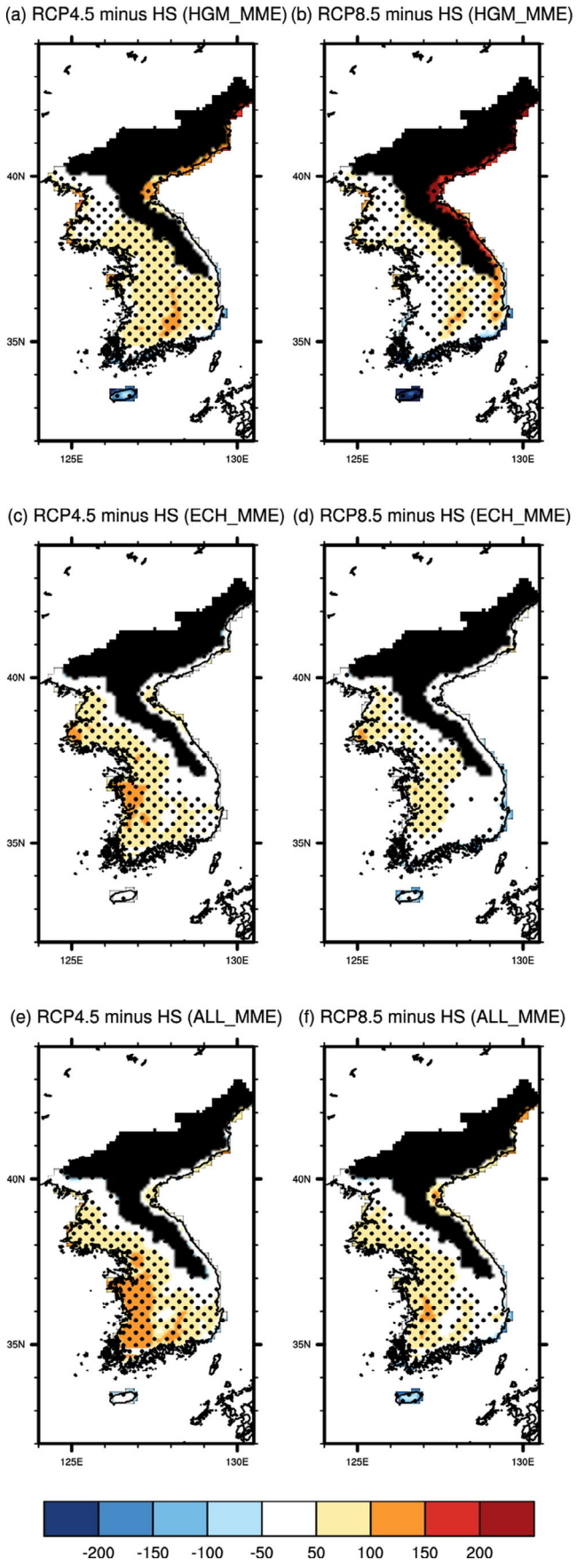

FIGURE 9 Legend on next page.

RCP4.5_CYP (Figure 9e) increases in the western and southern parts and northeastern coastal regions of the Korean Peninsula. Especially, it increases by more than 100 kg/10^{3}m^2 in the southwestern regions, including the major granary of South Korea. In the other regions, there are no significant changes in the maximum of RCP4.5_CYP. On the other hand, the maximum of RCP8.5_CYP (Figure 9f) increases in the western and northeastern coastal regions of the Korean Peninsula. The maximum of RCP8.5_CYP decreases in the southeastern coastal regions of the Korean Peninsula and Jeju Island and there are no significant changes in the maximum of RCP8.5_CYP in other regions. According to our analysis, the rice production in the Korean Peninsula for the optimum heading date is projected to increase in the western, southern and northeastern coastal regions of the Korea Peninsula and to decrease in the southeastern coastal regions and Jeju Island.

The differences in TS.CYP and DS.CYP for the optimum heading date between HS and RCPs (RCPs minus HS results) derived from ALL_MME (Figure 10) are also examined. First, there are no changes in TS.CYP (Figure 10a,b) in the western, southern and northeastern coastal areas of the Korean Peninsula where the maximum of CYP increases, but it increases in the southeastern coastal regions and Jeju Island where the maximum of CYP decreases and in some parts of the eastern regions where the maximum of CYP does not change. For RCP4.5, DS.CYP (Figure 10c) increases in most areas. Especially it increases by more than 25 hr in the southwestern regions where maximum CYP increases more than in other regions. For RCP8.5, DS.CYP (Figure 10d) increases in most of the areas except the southeastern regions of the Korean Peninsula where maximum CYP does not change. In summary, maximum CYP increases in the western and southern regions and northeastern coastal regions of the Korean Peninsula where TS.CYP does not change and DS.CYP increases. Maximum CYP decreases in the southeastern coastal regions of the Korean Peninsula and Jeju Island where both TS.CYP and DS.CYP increase. Maximum CYP does not change in the eastern part of the Korean Peninsula where both DS.CYP and TS.CYP increase or do not change. Maximum CYP increases when TS.CYP does not change and DS.CYP increases in the southern, western and northeastern coastal parts of the Korean Peninsula. However, CYP

FIGURE 9 Differences in maximum CYP (kg/10^3 m^2) during the heading date between HS and RCPs. The left (right) panels indicate the differences between the HS and RCP4.5 (RCP8.5) runs. Grid points with black dots show the 95% confidence level based on the Student's *t* test [Colour figure can be viewed at wileyonlinelibrary.com]

decreases or does not change when DS.CYP also increases but TS.CYP increases in Jeju Island and the eastern and southwestern coastal regions of the Korean Peninsula. As in mean CYP, maximum CYP is more affected by TS.CYP than by DS.CYP.

4 | SUMMARY AND CONCLUSION

In this study, the rice production in the Korean Peninsula (33–43°N, 124.5–130°E) in the near future (2021–2050) is projected under HS, RCP4.5 and RCP8.5 scenarios produced by three kinds of RCMs (WRF, MM5, GRIMs) with the initial and lateral forcing coming from two GCMs (HadGEM2-AO, ECHAM6) for more reliable estimation of rice production by reducing the uncertainty of prediction with finer resolution.

For this purpose, the dynamically downscaled daily temperature and daily sunshine duration are used to calculate the CYP index for Japonica-type rice. The results show that in spite of the extended possible period of rice ripening (CYP > 0), the average rice production decreases during the near future period, and also when the heading date is selected as the optimum heading date of HS. However, if the heading date is selected based on the optimum heading date of future climate (RCPs), which will be 12 days later (based on ALL_MME) than that of the HS, the rice production is expected to increase. This study finding therefore indicates that the rice production can increase in the near future (2021–2050) depending on the choice of the optimum heading date. In South Korea, the rice production is expected to increase if the optimum heading date is selected approximately 12 days later than the HS in the near future. However, according to Ahn *et al.* (2016), it will decrease in the far future because the maximum of RCPs_CYP is lower than that of HS_CYP during 2071–2100.

In order to estimate the future regional changes in CYP, the spatial distribution of mean CYP changes during the possible period of rice ripening is analysed. In ALL_MME, CYP increases by about 52.0 kg/10^3m^2 for RCP4.5 and 74.2 kg/10^3m^2 for RCP8.5 as TS.CYP decreases and DS.CYP increases. Therefore, mean rice production during the heading date of the near future is about 104% for RCP4.5 and 106% for RCP8.5 of that of the HS in the northeastern regions of the Korean Peninsula. In the western and southern regions of the Korean Peninsula and Jeju Island, CYP decreases by about 61.2 kg/10^3m^2 for RCP4.5 and 89.8 kg/10^3m^2 for RCP8.5 as TS.CYP increases and DS.CYP increases, or it does not change. Therefore, mean rice production during the heading date of the near future is about 95% for RCP4.5 and 93% for RCP8.5 of that of the HS in these regions. These results indicate that the mean rice production during the possible period of rice ripening increases in the northeastern coastal regions of the Korean Peninsula and decreases in the western and southern regions of the

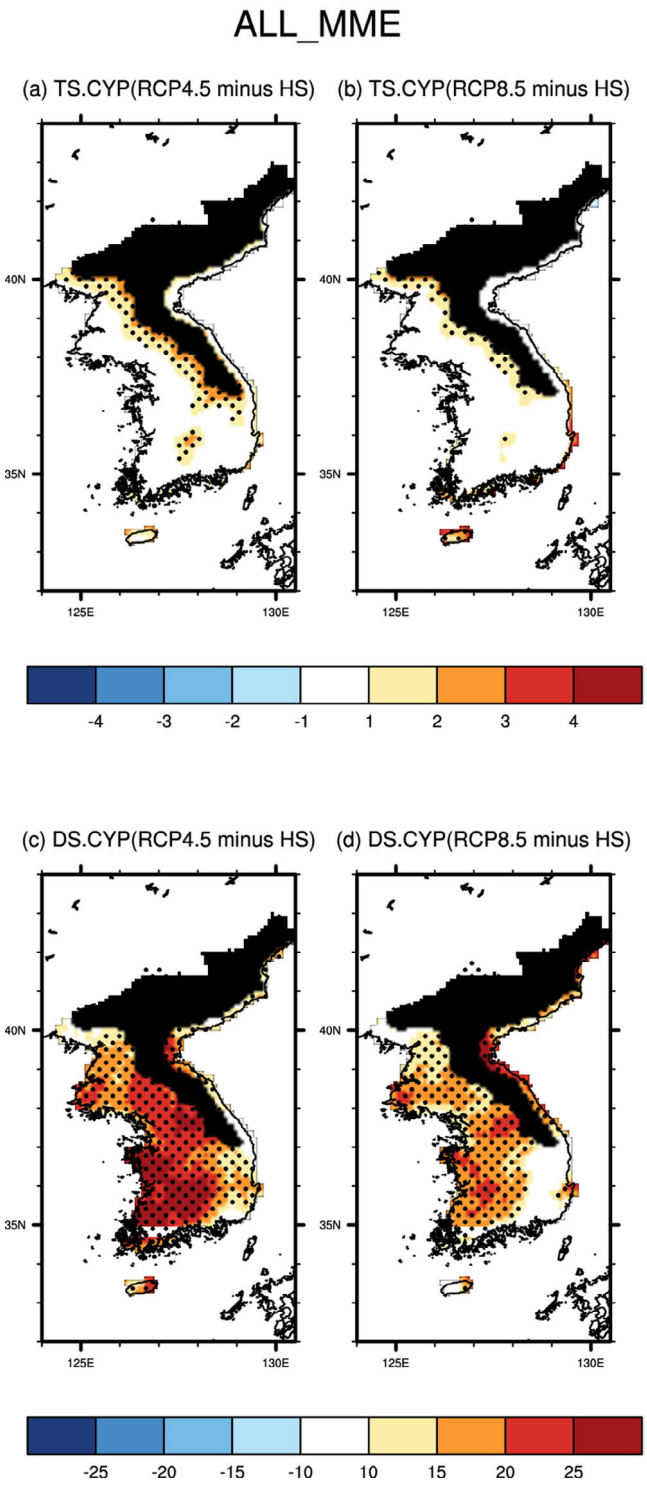

FIGURE 10 Differences in TS.CYP (°C) and DS.CYP (hr) when CYP is a maximum between HS and RCPs. The left (right) panels indicate the differences between the HS and RCP4.5 (RCP8.5) runs. eGrid points with black dots denote the 95% confidence level based on the Student's *t* test [Colour figure can be viewed at wileyonlinelibrary.com]

Korean Peninsula and Jeju Island. Especially, rice production decreases in South Korea will be more pronounced in the southwestern granary regions.

In addition, changes in the spatial distribution of maximum CYP for the optimum heading date are analysed. For ALL_MME, CYP increases by about 68.7 kg/10^{3}m^2 for RCP4.5 and 55.4 kg/10^{3}m^2 for RCP8.5 as TS.CYP does not change significantly and DS.CYP increases in the western, southern and northeastern coastal regions of the Korean Peninsula. Therefore, the peak rice production in the near future is expected to be about 105% for RCP4.5 and 104% for RCP8.5 of that in the HS. CYP is projected to decrease by about 29.7 kg/10^{3}m^2 for RCP4.5 and 55.1 kg/10^{3}m^2 for RCP8.5 as both TS.CYP and DS.CYP increase in the southeastern coastal regions of the Korean Peninsula and Jeju Island. Therefore, the peak rice production in the near future will be about 98% for RCP4.5 and 96% for RCP8.5 of that in the HS. These indicate that the peak rice production increases in the western, southern and northeastern coastal regions of the Korean Peninsula and decreases in the southeastern coastal regions of the Korean Peninsula and Jeju Island. Further, the difference between surface air temperature (T_a) and the most proper mean temperature (T_1) exerts a stronger effect on rice production than the sunshine duration does. Both mean CYP and maximum CYP decrease when the difference between T_a and T_1 increases, because the temperature affects the physiology of rice, such as the photosynthesis, respiration, water absorption, and nutrient absorption that are associated with rice growth (Han, 2016). As the temperature rises, rice production and quality are reduced by reducing spikelet fertility, shortening the growth period by increasing the rate of rice growth and increasing respiration during the ripening period (Horie, 1993; Chung, 2010; Lee *et al*., 2012c; Hong *et al*., 2018).

The limitation of the current study is the lack of consideration for other factors affecting rice production in the Korean Peninsula, such as agricultural damage caused by extreme weather phenomena (Song *et al*., 2012; Shim *et al*., 2013), the reduction of agricultural land due to urbanization (Lee *et al*., 2012a), the increase of disease occurrence under global warming (Shim *et al*., 2008b; Jeong *et al*., 2014), the change in the beginning and ending times of the monsoon (Changma), the increase in the intensity of rainfall due to climate change (Hong and Ahn, 2015), and the improvement of species adapted to climate change (Ku *et al*., 2014;Shin *et al*., 2013). Thus, accounting for these factors in future studies will give a more reliable prediction of future rice production.

ACKNOWLEDGEMENTS

This work was carried out with the support of the Korea Meteorological Administration Research and Development Program under Grant KMI2018-01213 and "Cooperative Research Program for Agriculture Science & Technology Development (Project No. PJ01489102)" Rural Development Administration, Republic of Korea.

ORCID

Joong-Bae Ahn https://orcid.org/0000-0001-6958-2801
Young-Hyun Kim https://orcid.org/0000-0001-6046-3873
Dong-Hyun Cha https://orcid.org/0000-0001-5053-6741
Seung-Ki Min https://orcid.org/0000-0002-6749-010X

REFERENCES

Ahn, J.B., Choi, Y.W., Jo, S.R. and Hong, J.Y. (2014) Projection of 21st century climate over Korean peninsula: temperature and precipitation simulated by WRFV3.4 based on RCP4.5 and 8.5 scenarios. *Atmosphere*, 24(4), 541–554.

Ahn, J.B., Hong, J.Y. and Shim, K.M. (2016) Agro-climate changes over Northeast Asia in RCP scenarios simulated by WRF. *International Journal of Climatology*, 36, 1278–1290. https://doi.org/10.1002/joc.4423.

Bancy, M.M. (2000) The influence of climate change on maize production in the semi-humid-semi-arid areas of Kenya. *Journal of Arid Environments*, 46, 333–344. https://doi.org/10.1006/jare.2000.0699.

Chen, H. and Sun, J. (2013) Projected change in east Asian summer monsoon precipitation under RCP scenario. *Meteorology and Atmospheric Physics*, 121, 55–77.

Choi, H.C. (2002) Current status and perspectives in varietal improvement of rice cultivars for high-quality and value-added products. *Korean Journal of Crop Science*, 47, 15–32.

Chung, S.O. (2010) Simulating evapotranspiration and yield responses of rice to climate change using FAO-AquaCrop. *Journal of the Korean Society of Agricultural Engineers*, 52(3), 57–64.

Collins, W.J., Bellouin, N., Doutriaux-Boucher, M., Gedney, N., Halloran, P., Hinton, T., Hughes, J., Jones, C.D., Joshi, M., Liddicoat, S., Martin, G., O'Connor, F., Rae, J., Senior, C., Sitch, S., Totterdell, I., Wiltshire, A. and Woodward, S. (2011) Development and evaluation of an earth-system model—HadGEM2. *Geoscientific Model Development*, 4, 1051–1075.

Deressa, T.T. and Hassan, R.M. (2009) Economic impact of climate change on crop production in Ethiopia: evidence from cross-section measures. *Journal of African Economies*, 18(4), 529–554.

FAO. (2016) Crop prospects and food situation, No. 4. http://www.fao.org/giews/reports/crop-prospects/en/.

Gao, X.J., Wang, M.L. and Giorgi, F. (2013) Climate change over China in the 21st century as simulated by BCC_CSM1.1-RegCM4.0. *Atmospheric and Oceanic Science Letters*, 6, 381–386. https://doi.org/10.3878/j.issn.1674-2834.13.0029.

Gitz, V., Meybeck, A., Lipper, L., Young, C. and Braatz, S.. (2016) *Climate change and food security: Risks and responses.* Rome, Italy. Food and Agriculture Organization, www.fao.org/3/a-i5188e.pdf.

Han, S.H. (2016) A study of building Rice crop yield forecasting model. *Journal of Agriculture and Life Science*, 50(3), 219–229.

Hanyu, J., Uchijima, T. and Sugawara, S. (1966) Studies on the agro-climatological method for expressing the paddy rice products. I. an agro-climatic index for expressing the quantity of ripening of the paddy rice. *Bulletin of Tohoku National Agricultural Experimental Station*, 34, 27–36.

Hong, J.Y. and Ahn, J.B. (2015) Changes of early summer precipitation in the Korean peninsula and nearby regions based on RC P simulations. *Journal of Climate*, 28, 3557–3578.

Hong, S.Y., Oh, S.G., Suh, M.S., Lee, D.K., Ahn, J.B. and Kang, H.S. (2013a) Future climate changes over north-east Asian region simulated by RegCM4 based on the RCP scenarios. *Journal of Climate Research*, 8(1), 27–44.

Hong, S.Y., Park, H., Cheong, H.B., Kim, J.E.E., Koo, M.S., Jang, J., Ham, S., Hwang, S.O., Park, B.K., Chang, E.C. and Li, H. (2013b) The global/regional integrated model system (GRIM). *Asia-Pacific Journal of Atmospheric Sciences*, 49(2), 219–243. https://doi.org/10.1007/s13143-013-0023-0.

Hong, S.C., Hur, S.O., Choi, S.K., Choi, D.H. and Jang, E.S. (2018) Elevated temperature treatment induced rice growth and changes of carbon content in Paddy water and soil. *Korean Journal of Environment Agriculture.*, 37(1), 15–20.

Horie, T. (1993) Predicting the effects of climatic variation and elevated CO_2 on rice yield in Japan. *Journal of Agricultural Meteorology*, 48, 567–574.

Hur, J.N., Ahn, J.B. and Shim, K.M. (2017) Assessment and prediction of the first-flowering dates for the major fruit trees in Korea using a multi-RCM ensemble. *International Journal of Climatology*, 37, 1603–1618.

Intergovernmental Panel on Climate Chage (IPCC). (2013, 1535) Climate change 2013: the physical science basis. In: Stocker, T.F., Qin, D., Plattner, G.K., Tignor, M., Allen, S.K., Boschung, J., Nauels, A., Xia, Y., Bex, V. and Midgley, P.M. (Eds.) *Contribution of Working Group I to the Fifth Assessment Report of the Intergovernmental Panel on Climate Change*. Cambridge and New York: Cambridge University Press.

Jeong, H.K., Kim, C.G. and Moon, D.H. (2014) An analysis of impacts of climate change on rice damage occurrence by insect pests and disease. *Korean Journal of Environmental Agriculture*, 33(1), 52–56.

Jeong, O.Y., Torollo, G., Bombay, M., Baek, M.K., Ahn, E.K., Hyun, W.J., Park, H.S., Jeong, J.M., Cho, J.H., Lee, J.H., Yeo, U.S., Lee, J.S., Jeong, E.G., Kim, C.S., Suh, J.P., Kim, B.K. and Lee, J.H. (2019) Adaptable tropical japonica high quality new Rice cultivar 'japonica 6'. *The Journal of the Korean Society of International Agriculture*, 31(3), 249–254.

Kim, J. (2010) Modeling the effects of temperature, solar radiation and leaf senescence on grain filling of rice. Ph. D. thesis. Seoul National University, Seoul.

Kim, C.S., Lee, J.S., Ko, J.Y., Yun, E.S., Yeo, U.S., Lee, J.H., Kwak, D.Y., Shin, M.S. and Oh, B.G. (2007) Evaluation of optimum rice heading period under recent climatic change in Yeongnam area. *Korean Journal of Agricultural and Forest Meteorology*, 9, 17–28.

Kim, D.J., Roh, J.H., Kim, J.G. and Yun, J.I. (2013) The influence of shifting planting date on cereal grains production under the projected climate change. *Korean Journal of Agricultural and Forest Meteorology*, 15(1), 26–39.

Ku, B.I., Kang, S.K., Sang, W.G., Lee, M.H., Park, H.K., Kim, Y.D. and Lee, J.H. (2014) Study of rice double cropping feasibility in Korea to cope with climate change. *Journal of Agriculture & Life Science*, 45(1), 39–46.

Lee, D.K., Cha, D.H. and Kang, H.S. (2004) Regional climate simulation for the 1998 summer flood over East Asia. *Journal of the Meteorological Society of Japan*, 82, 1735–1753. https://doi.org/10.2151/jmsj.82.1735.

Lee, B.S., Hong, S.W., Kang, H.J., Lee, J.S., Yun, S.T. and Nam, K.P. (2012a) Groundwater recharge and discharge in the urban-rural composite area. *Journal of Soil and Groundwater Environment*, 17(2), 37–46.

Lee, C.K., Kim, J., Shon, J., Yang, W.H., Yoon, Y.H., Choi, K.J. and Kim, K.S. (2012b) Impacts of climate change on rice production and adaptation method in Korea as evaluated by simulation study. *Korean Journal of Agricultural and Forest Meteorology*, 14, 207–221. https://doi.org/10.5532/KJAFM.2012.14.4.207.

Lee, T.S., Choi, J.Y., Yoo, S.H., Lee, S.H. and Oh, Y.G. (2012c) Analyzing consumptive use of water and yields of Paddy Rice by climate change. *Journal of the Korean Society of Agricultural Engineers*, 54(1), 47–54.

Lee, D.J., Kim, J.H. and Kim, K.S. (2014) Spatiotemporal assessment of the late marginal heading date of Rice using climate Normal data in Korea. *Korean Journal of Agricultural and Forest Meteorology*, 16(3), 316–326.

Lee, S.H., Son, E.H., Hong, S.C., Oh, S.H., Lee, J.Y., Park, J.H., Woo, S.H. and Lee, C.W. (2016) Growth and yield under low solar radiation during the reproductive growth stages of Rice plants. *Korean Journal of Crop Science*, 61(2), 87–91.

Masutomi, Y., Takahashi, K., Harasawa, H. and Matsuoka, Y. (2009) Impact assessment of climate change on rice production in Asia in comprehensive consideration of process/parameter uncertainty in general circulation models. *Agriculture, Ecosystems and Environment*, 131, 281–291.

Matthews, R.B., Kropff, M.J., Horie, T. and Bachelet, D. (1997) Simulating the impact of climate change on Rice production in Asia and evaluating options for adaptation. *Agricultural Systems*, 54(3), 399–425.

Oh, S.G., Park, J.H., Lee, S.H. and Suh, M.S. (2014) Assessment of the RegCM4 over East Asia and future precipitation change adapted to the RCP scenarios. *Journal of Geophysical Research-Atmospheres*, 119, 2913–2927.

Park, H.S., Baek, M.K., Nam, J.K., Shin, W.C., Lee, G.M., Park, S. G., Lee, C.M., Kim, C.S., Cho, Y.C. and Kim, B.K. (2017) Development and characterization of breeding materials with diverse grain size and shape in japonica Rice. *Korean Journal of Breeding Science*, 49(4), 369–389.

Park, H.S., Baek, M.K., Nam, J.K., Shin, W.C., Lee, G.M., Park, S.G., Lee, C.M., Kim, C.S. and Cho, Y.C. (2018) Development and characterization of japonica Rice line with long and spindle-shaped grain. *Korean Journal of Breeding Science*, 50(2), 116–130.

Parry, M.L., Rosenzweig, C., Iglesias, A., Livermore, M. and Fischer, G. (2004) Effects if climate change on global food production under SRES emissions and socio-economic scenarios. *Global Environmental Change*, 14, 53–67.

Peng, S., Huang, J., Sheehy, J.E., Lasa, R.C., Visperas, R.M., Zhong, X., Centeno, G.S., Khush, G.S. and Cassman, K.G. (2004) Rice yields decline with higher night temperature from global warming. *Proceedings of the National Academy of Sciences of the United States of America*, 101(27), 9971–9975.

RDA. (2004) The Production of High Quality Rice and Quality Control. Rural Development Administration: 283 (in Korean)

RDA. (2019) *Weekly Farming Information*. South Korea: Rural Development Administration.

Seo, Y.H., Lee, A.S., Cho, B.O., Kang, A.S., Jeong, B.C. and Jung, Y. S. (2010) Adaptation study of Rice cultivation in Gangwon Province to climate change. *Korean Journal of Agricultural and Forest Meteorology*, 12(2), 143–151.

Shim, K.M., Kim, G.Y., Roh, K.A., Jeong, H.C. and Lee, D.B. (2008a) Evaluation of agro-climatic indices under climate change. *Korean Journal of Agricultural and Forest Meteorology*, 10(4), 113–120.

Shim, K.M., Kim, G.Y., Jeong, H.C. and Lee, J.T. (2008b) Adaptation and assessment of the impacts of global warming on agricultural environment in Korea. *Proceedings of the Korean Society for Bio-Environment Control Conference*, 17(1), 78–81.

Shim, K.M., Kim, Y.S., Jung, M.P., Kim, S.C., Min, S.H. and So, K.H. (2013) Agro-climatic zonal characteristics of the frequency of abnormal air temperature occurrence in South Korea. *Korean Journal of Agricultural and Forest Meteorology*, 4(2), 189–199.

Shin, G.H., Ko, A.Y., Kim, D.B., Lee, Y.J. and Lee, O.H. (2013) Physicochemical characteristics of onion with cold tolerance cultivated in Kangwon. *Korean Journal of Food Preservation*, 20(6), 894–898.

Son, Y, Lee, H.W., Kim, S.Y., Hwang, D.Y., Park, S.T., Yang, S.J. (2002) Relationship of climatic factors to rice yield in different area. Yeongnam Agricultural Research Institute research report: pp. 162–172.

Song, I.H., Song, J.H., Kim, S.M., Jang, M.W. and Kang, M.S. (2012) Spatial distribution and regional characteristics of meteorological damages to agricultural farms in Korea. *Journal of Korean Society of Agricultural Engineers*, 54(6), 45–52.

Stevens, B., Giorgetta, M., Esch, M., Mauritsen, T., Crueger, T., Rast, S., Salzmann, M., Schmidt, H., Bader, J., Block, K., Brokopf, R., Fast, I., Kinne, S., Kornblueh, L., Lohmann, U., Pincus, R., Reichler, T. and Roeckner, E. (2013) Atmospheric component of the MPI-M earth system model: ECHAM6. *Journal of Advances in Modeling Earth Systems*, 5(2), 146–172.

Tebaldi, C. and Knutti, R. (2007) The use of the multi-model ensemble in probabilistic climate projections. *Philosophical Transactions of the Royal Society A*, 365(1857), 2053–2075.

USDA. (2009) World Agricultural Supply and Demand Estimates, WASDE-468.

Van Oort, P.A.J. and Zwart, S.J. (2017) Impacts of climate change on rice production in Africa and causes of simulated yield changes. *Global Change Biology*, 24, 1029–1045.

Wang, H. and Hijmans, R.J. (2019) Climate change and geographic shifts in rice production in China. *Environmental Research Communications*, 1(1), 011008.

Wang, W., Ding, Y., Shao, Q., Xu, J., Jiao, X., Luo, Y. and Yu, Z. (2017) Bayesian multi-model projection of irrigation requirement and water use efficiency in three typical rice plantation region of China based on CMIP5. *Agricultural and Forest Meteorology*, 232, 89–105.

Wei, X., Jiang, L., Xu, J., Zhang, W., Lu, G., Zhang, Y. and Wan, J. (2008) Genetic analyses of heading date of japonica rice cultivars from Northeast China. *Field Crops Research*, 107(2), 147–154. https://doi.org/10.1016/j.fcr.2008.01.008.

Wei, X.J., Jiang, L., Xu, J.F., Liu, X., Liu, S.J., Zhai, H.Q. and Wan, J.M. (2009) The distribution of japonica rice cultivars in the lower region of the Yangtze River valley is determined by its photoperiod-sensitivity and heading date genotypes. *Journal of Integrative Plant Biology*, 51(10), 922–932. https://doi.org/10.1111/j.1744-7909.2009.00866.x.

World food Programme (WFP). (2016) 2017 WFP Year in Review.

Zhao, G., Webber, H., Hoffmann, H., Wolf, J., Siebert, S. and Ewert, F. (2015) The implication of irrigation in climate change impact assessment: a European-wide study. *Global Change Biology*, 21(11), 4031–4048.

How to cite this article: Ahn J-B, Kim Y-H, Shim K-M, *et al.* Climatic yield potential of Japonica-type rice in the Korean Peninsula under RCP scenarios using the ensemble of multi-GCM and multi-RCM chains. *Int J Climatol*. 2020;1–16. https://doi.org/10.1002/joc.6767